

# UC Berkeley

## Technical Completion Reports

### Title

Development of a decadal-scale estuarine geomorphic model for Suisun Bay, California: calibration, validation, and idealized time-stepping

### Permalink

<https://escholarship.org/uc/item/7cc2j5x6>

### Authors

Ganju, Neil K  
Schoellhamer, David H  
Younis, Bassam A

### Publication Date

2006-08-01

Development of a decadal-scale  
estuarine geomorphic model  
for Suisun Bay, California: calibration,  
validation, and idealized time-stepping

Neil K. Ganju, [nganju@usgs.gov](mailto:nganju@usgs.gov)  
David H. Schoellhamer, [dschoell@usgs.gov](mailto:dschoell@usgs.gov)  
Bassam A. Younis, [bayounis@ucdavis.edu](mailto:bayounis@ucdavis.edu)

Civil and Environmental Engineering Department  
University of California, Davis  
One Shields Avenue, Davis, California 95616

UC Water Resources Center  
Technical Completion Report Project No. W-991  
August, 2006

## **Abstract**

Geomorphic evolution of estuarine habitats and landscapes over decadal timescales (>10 years) is sensitive to sediment supply from the watershed as well as estuarine hydrodynamics. Sediment supply to Suisun Bay, California is subject to natural as well as anthropogenic influence, beginning with the drastic input of sediment during the hydraulic mining period of the late 19<sup>th</sup> century. Today sediment supply is declining due to reduction of the hydraulic mining sediment pulse, reservoir storage, and land use practices. Future climate change, land use change, and sea level rise are some of the many factors that may alter sediment supply and threaten ecologically beneficial estuarine habitats. We have developed an estuarine geomorphic model based on a traditional tidal timescale hydrodynamic/sediment transport model, by idealizing boundary conditions, applying novel calibration procedures, and implementing a simplified time-stepping method. The Regional Oceanic Modeling System (ROMS) was developed for Suisun Bay, for the purpose of hindcasting historical geomorphic change and modeling future scenarios of geomorphic change. Seaward boundary conditions were idealized using tidal harmonic prediction for tidal stage and velocity, and a synthetic time-series for sediment concentrations was constructed by applying typical seasonal wind patterns and the spring-neap tidal signal. Calibration of these idealized boundary conditions and bed sediment parameters was accomplished using sediment flux data for the boundaries of Suisun Bay from water years 1997 and 2004. Calibrating to sediment fluxes guarantees that modeled net geomorphic change will not exceed the total supply of sediment from landward and seaward sources. The successful simulations of 1997 and 2004 allow for the development of a time-stepping method that reduces computational expense. The method involves simulating the two distinct sediment-transport seasons of Suisun Bay as month-long periods, then extrapolating the results of each compressed period for the entire season. Computational time for hindcasting and future scenario simulations is now reduced by 85% using this simplified method.

## **Introduction and Problem Statement**

California's delicate balance between water supply and ecosystem preservation is under increasing pressure from a growing population and habitat loss. The locus of many of these issues is San Francisco Bay, where freshwater from the Sacramento/San Joaquin Delta meets saline water from the Pacific Ocean. Suisun Bay is the furthest landward subembayment of San Francisco Bay, and is therefore most responsive to freshwater flow. Water withdrawals from the Delta adversely impact the estuarine ecosystem and habitats. Increasing the quality of habitat in Suisun Bay, however, would decrease the ecosystem stress caused by freshwater flow diversions. Current goals of ecosystem restoration include the creation and maintenance of beneficial wetlands and shallow-water habitat (Goals Project 1999).

Geomorphic evolution of estuarine habitats and landscapes over decadal timescales (>10 years) is sensitive to sediment supply from the watershed as well as estuarine hydrodynamics. Sediment supply to the Bay is an ongoing issue, beginning with the drastic input of sediment during the hydraulic mining period of the late 19<sup>th</sup> century (Gilbert 1917). Today sediment supply is declining due to reduction of the hydraulic mining sediment pulse, reservoir storage, and land use practices (Wright and Schoellhamer 2004). Future climate change, land use change, and sea level rise are some

of the many factors that may alter sediment supply and threaten ecologically beneficial estuarine habitats (Scavia et al. 2002, Pont et al. 2002). Hydrodynamics are directly modulated by the varying morphology of the Bay (and vice-versa), so there is a feedback between hydrodynamics and geomorphology.

## **Objectives**

The specific objectives of the research were as follows:

1. Develop a tidal timescale hydrodynamic/sediment transport model of Suisun Bay based on existing public-domain software.
2. Implement idealized boundary conditions for the seaward boundary of the domain, due to the lack historical data for hindcasting simulations.
3. Calibrate and validate the complete model with reference to sediment flux data at the landward and seaward boundaries of Suisun Bay from 1997 and 2004 (McKee et al. 2006; Ganju and Schoellhamer in press).
4. Evaluate the accuracy of a time-stepping procedure which simulates hydrologic seasons as separate periods, and extrapolates the results for the entire water year.
5. Develop historically based landward boundary conditions for hindcasting simulations based on the historical geomorphic data from Cappiella et al. (1999).

## **Procedure**

### Site description

Our study area is Suisun Bay, the most landward subembayment of northern San Francisco Bay (Figs. 1, 2). The Sacramento and San Joaquin Rivers deliver freshwater to Suisun Bay, primarily during the winter rainy season and during the spring snowmelt and reservoir releases. Precipitation is negligible during late spring and summer. Suisun Bay is a partially mixed estuary that has extensive areas of shallow water that are less than 2 m deep at mean lower-low water. Shallow estuarine environments such as Suisun Bay are ecologically significant because a large fraction of the biota depends on these areas for shelter and nourishment (Cloern et al. 1985, Caffrey et al. 1998). Wetlands, which usually form on shallow fringes of the Bay, provide habitat for species and communities not found elsewhere within the Bay (Goals Project 1999). Channels in Suisun Bay are about 9-11 m deep. Carquinez Strait is a narrow channel about 18 m deep that connects Suisun Bay to San Pablo Bay, to the rest of San Francisco Bay, and to the Pacific Ocean. Tides are mixed diurnal and semidiurnal and the tidal range varies from about 0.6 m during the weakest neap tides to 1.8 m during the strongest spring tides. Freshwater inflow typically first encounters saltwater in the lower rivers, Suisun Bay, and Carquinez Strait. The salinity range in this area is about 0-25 and depends on freshwater inflow.

Suspended and bed sediment in Suisun Bay is predominately fine and cohesive, except for sandy bed sediment in some of the deeper channels (Conomos and Peterson 1977). The typical suspended-sediment concentration (SSC) range in northern San Francisco Bay is about 10-300 mg/L and sometimes up to about 1,000 mg/L in an estuarine turbidity maximum (ETM). In Suisun Bay, ETMs are located near sills and sometimes near a salinity of 2, depending on tidal phase and the spring/neap tidal cycle

(Schoellhamer and Burau 1998, Schoellhamer 2001a). Accumulations of suspended sediment, nutrients, phytoplankton, zooplankton, larvae, and juvenile fish are found in ETMs (Peterson et al. 1975, Arthur and Ball 1979, Kimmerer 1992, Jassby and Powell 1994, Schoellhamer and Burau 1998). The location of a bottom salinity of 2 is used as a habitat indicator to regulate freshwater flow to the Bay because it is believed to be an easily measured indicator of the location of the ETM and a salinity preferred by many estuarine species (Jassby et al. 1995).

An annual cycle of sediment delivery and redistribution begins with large influx of sediment during winter (delivery), primarily from the Central Valley (Goodwin and Denton 1991, McKee et al. 2006). Much of this new sediment deposits in San Pablo and Suisun Bays. Stronger westerly winds during spring and summer cause wind-wave resuspension of bottom sediment in these shallow waters and increase SSC (Ruhl and Schoellhamer 2004). The ability of wind to increase SSC is greatest early in the spring, when unconsolidated fine sediments can easily be resuspended. As the fine sediments are winnowed from the bed, however, the remaining sediments become progressively coarser and less erodible (Conomos and Peterson 1977; Krone 1979; Ruhl and Schoellhamer 2004). Thus, tides and wind redistribute the annual pulse of new sediment throughout the Bay. Since 1850, alterations in the watershed and estuary have changed the bathymetry of Suisun Bay (Cappiella et al. 1999, Fig. 3).

### Model development

The Regional Oceanic Modeling System (Shchepetkin and McWilliams, 2005) is a public-domain hydrodynamic model with an optional sediment transport module. There are several advantages that ROMS has over other available models: 1) it is free, public-domain software (which is tens of thousands dollars cheaper than most models); 2) it is improved and expanded amongst hundreds of researchers continuously; and 3) it is part of a community-based sediment transport initiative by the U.S. Geological Survey.

ROMS is a split-mode model: the barotropic, depth-integrated equations are solved on a shorter (fast) time step (due to barotropic propagation speed) while the baroclinic terms are solved at a longer (slow) time step. The grid features of ROMS are: an Arakawa “C” grid, orthogonal curvilinear horizontal coordinates (Fig. 4), and stretched, terrain-following vertical coordinate. Boundary conditions for momentum/tracers on the four edges of the grid can be clamped (fixed), gradient (zero-derivative), radiation (allow disturbances to propagate away), or wall (zero-flux). In all cases, ROMS has adaptive capabilities, in order to switch from active conditions for inward fluxes and passive conditions for outward fluxes. Discretization options for momentum/tracers range from the 2nd order to 4th order (in space). With regards to turbulence, at least four common two-equation closures (k-epsilon, k-kl, k-omega, and gen) can be specified with the generic length scale implementation provided in the model. Sediment transport in the form of both suspended and bed load (Meyer-Peter Muller version) has been implemented in the latest version of ROMS (<http://marine.rutgers.edu/po/index.php?model=roms>)

### Modeling domain

The domain of Suisun Bay is discretized in the orthogonal, curvilinear system used by ROMS (Fig. 4). This is accomplished using the freely available Seagrid toolkit

([http://woodshole.er.usgs.gov/staffpages/cdenham/public\\_html/seagrid/seagrid.html](http://woodshole.er.usgs.gov/staffpages/cdenham/public_html/seagrid/seagrid.html)).

Required inputs are: 1) a coastline file that consists of ordered pairs of latitude and longitude coordinates that form the coastline, 2) a bathymetry file that consists of multiple sets of corresponding latitude, longitude, and depth values, and 3) a boundary file that specifies the four corner points of the modeled domain. The Seagrid program allows the user to choose the number of rows and columns within the domain, with default even spacing along the domain boundaries. The coastline file was obtained from the National Geophysical Data Center ([www.ngdc.noaa.gov](http://www.ngdc.noaa.gov)), while the bathymetry file was produced using data from Cappiella et al. (1999). Latitudes and longitudes from the Cappiella et al. (1999) data set were converted from UTM zone 10 format to degree/minute/second format using the U.S. Army Corps of Engineer's Corpscon program.

Though Mallard Island is the geographic landward boundary of Suisun Bay, specifying boundary conditions at this location for historical and future multi-decadal simulations is difficult. Bidirectional flow is observed more than 50 km upstream of Mallard Island. Prescribing flow, salinity, and suspended-sediment concentrations at the Mallard Island boundary is possible for simulating recent periods, but data do not exist for periods prior to the late 20<sup>th</sup> century. Therefore extending the boundary to the bidirectional flow limit simplifies specification of boundary conditions. For instance, unidirectional freshwater flow measurements exist from 1929 onwards, and prior flows can be estimated using various proxies. Salinity can be specified as zero, and sediment loads can be estimated with rating curves for the Sacramento and San Joaquin Rivers.

Extending the landward boundary poses one major problem: the Sacramento/San Joaquin Delta represents a complex domain with multiple channels, open-water areas, flow gates, and export pumps. Including the Delta would increase the modeling domain by over 100%, and require extensive calibration for in-Delta hydrodynamic processes. Therefore we simplify the Delta in this study, as a single, continuous channel. The channel has the same water surface area as the Delta (and therefore tidal prism), and length equivalent to the distance from Mallard Island to Freeport (on the Sacramento River). Calibration of stage and salinity within the domain of Suisun Bay is unaffected by this idealization (Ganju and Schoellhamer, 2005).

Carquinez Strait, immediately landward of the Napa River, was chosen as the seaward boundary of the domain. Eastern Carquinez Strait is subject to complex circulation dynamics due to geometry of the Strait as well as baroclinic effects. Suspended-sediment dynamics near the I-680 Bridge are sensitive to the formation of an estuarine turbidity maximum on the north side of the Strait (Ganju and Schoellhamer 2005, Schoellhamer and Burau 1998). Inclusion of the Napa River was ruled out due to a lack of long-term sediment load data; therefore the logical seaward boundary was landward of the Napa River but seaward of the I-680 Bridge.

#### Idealization of landward boundary conditions: flow, salt, sediment

Net freshwater flow into Suisun Bay is a combination of flows through the Sacramento River, San Joaquin River, the ephemeral Yolo Bypass, minor tributaries, and exports by the federal and state water projects. Because these separate inputs and outputs are not explicitly modeled, the net flow is the parameter of interest. The DAYFLOW program (California Department of Water Resources) balances these inputs and outputs, to yield a daily value of flow past Mallard Island. This value is imposed at the landward

boundary of the domain. Conceptually, this ignores the within-Delta transfer of water (and therefore sediment). However, the model will be calibrated to fluxes at the Mallard Island cross-section, so actual sediment retention within the Delta system will be accurately represented (though possible sediment exports by the water projects will be ignored). Salinity at the landward boundary is specified as zero.

Daily sediment loads past Freeport on the Sacramento River and Vernalis on the San Joaquin River were obtained from the U.S. Geological Survey. For modeling purposes, the suspended-sediment concentration is specified as a boundary condition, therefore the loads are divided by the DAYFLOW value to yield the appropriate landward boundary SSC.

All boundary conditions are spread equally across the cells on the landward boundary, both vertically and laterally.

#### Idealization of seaward boundary conditions: tides, velocities, salt, sediment

Because the final geomorphic model will be used for simulations spanning the 19<sup>th</sup> and 20<sup>th</sup> centuries (when detailed data at the seaward boundary were not always available), idealizations are necessary in terms of tidal height, velocity, salinity, and SSC. Tidal harmonics provide an appropriate initial estimate of historic tidal elevations and velocities. A tidal harmonic predictor was developed through instrument deployments (Jeff Gartner, writ. comm.), for locations throughout San Francisco Bay. The predictor provides tidal elevations and velocities at the west end of Carquinez Strait, which is the seaward boundary of the modeled domain. While these values are imposed on the seaward boundary of the model, the actual boundary condition is not strictly clamped, and allows the tidal elevation and velocities to adjust to net outflow (from freshwater flow). Nonetheless, meteorological forcings such as wind and barometric pressure are not represented in the tidal record. The tidal elevation and depth-averaged velocity are applied uniformly in a lateral sense at the seaward boundary, while the 3D velocity field is solved with a gradient condition.

For salinity, the method of Warner et al. (2005) can be used, which utilizes a deterministic function based on near-bottom longitudinal salinity profiles as follows:

$$S(X) = (S_0/2) [1 + \tanh(\alpha - X/\beta)] \quad (1)$$

where  $S$  is the salinity in psu,  $X$  is the longitudinal coordinate with origin at the mouth of the estuary,  $S_0$  is the oceanic value of salinity (held at 30 psu), and  $\alpha$ ,  $\beta$  are empirical parameters. Parameter  $\alpha$  is held constant as 2 following Warner et al. (2005). The parameter  $\beta$  is related to freshwater flow; for a given estuary this relationship can be established and used in the expression. Data from 358 longitudinal cruises between 1969-2005 of the R/V *Polaris* were processed to determine this relationship (Figs. 5, 6). Within the model code, the salinity gradient is calculated as a function of freshwater flow. This salinity gradient is applied on flood tides, at the first interior point of the domain, to calculate the flood tide salinity. This function was shown to work adequately in prior simulations (Ganju and Schoellhamer 2005).

Sediment boundary conditions are substantially more difficult, as SSC at the seaward boundary responds to freshwater flow, tidal energy, wind-wave resuspension in San Pablo Bay. Schoellhamer (2001b) constructed synthetic SSC time-series as a means of testing spectral analysis routines; these time-series combined fluctuations in SSC due

to seasonal variability of winds, spring-neap tidal energy, and tidal advection. Because flood-tide SSC is the parameter of interest, the measured flood-tide SSC at Carquinez Bridge was averaged on a daily basis. The pattern for water years 2002, 2003, and 2004 showed a similar pattern: a seasonal pattern related to freshwater flow and wind-wave resuspension was superimposed on a spring-neap pattern that had greatest variability during high freshwater-flow periods and the least variability at the beginning and end of the water year (when sediment input is at a minimum). Therefore two signals were superimposed to recreate a synthetic time-series of SSC: a seasonal wind-wave signal that peaks in the summer, and a spring-neap signal that is a function of tidal energy (obtained from tidal harmonics) and the seasonal contributions. The time-series is then modulated by mean yearly SSC and a random fluctuation that is 10% of the SSC value. The mean yearly SSC at sites Car and PSP is linearly related to total sediment input from the Delta during the water year. This relationship suggests that despite significant tidal and atmospheric forcing, the net sediment input does affect baseline and average SSC throughout the Bay.

### Atmospheric forcing

The effect of wind-waves on sediment resuspension in San Francisco Bay can be substantial during episodic winter storm events and the diurnal winds during the summer. Wind data from site Met were used to calculate wave height and period using the Shore Protection Manual equation for fetch and depth-limited waves (Coastal Engineering Research Center 1984). Though fetch within Suisun Bay depends on wind direction and location, a uniform fetch of 20 km was assumed. Major wind events in Suisun Bay tend from a westerly direction, so wave direction was held constant at 270 degrees. Ultimately, wave period was also held constant, for simplicity. Though there are modern data available for implementing wind-waves in the model, there is still a need to construct a generic wind-wave time-series for historical simulations where data are not available. This is accomplished by specifying episodic winds before major flow peaks (congruent with the passage of Pacific storms) and diurnal winds for all other periods, with peak strength in the summer.

### Calibration to water year 1997 fluxes

The seaward suspended-sediment concentration boundary condition and sediment properties (i.e. bed shear strength, settling velocity, erosion rate) are calibrated to the water year 1997 data. This period contains peak freshwater flows that are 3.5 times greater than the 2004 period, and yearly cumulative flow is a factor of two larger. Therefore we will calibrate to a relatively extreme (in terms of freshwater flow) period, and the mechanics of the model will be validated during a drier period. Landward boundary conditions and the remaining seaward boundary conditions are specified as outlined above. Calibration goals are to simulate the correct net flux between Suisun Bay and the Delta (Mallard Island cross-section), and the correct net flux between Suisun Bay and Carquinez Strait (Benicia Bridge cross-section) within the error bounds of the flux measurements (McKee et al. 2006; Ganju and Schoellhamer in press).



### Validation to water year 2004 fluxes

The calibrated model is validated using flux data from water year 2004. Therefore we calibrate to a relatively dry period, and the mechanics of the model are validated during a much wetter period. Again, validation will be quantified in reference to simulating the correct net flux between Suisun Bay and the Delta (Mallard Island cross-section), and the correct net flux between Suisun Bay and Carquinez Strait (Benicia Bridge cross-section) within the error bounds of the flux measurements (McKee et al. 2006; Ganju and Schoellhamer in press).

### Formulation of time-stepping procedure

Analysis of model results suggests that fluxes over the most dynamic periods (winter, summer) can be extrapolated individually to represent seasonal dynamics accurately. This procedure was tested for the two modeled water years. Two four-week periods were selected to represent 1) winter conditions (high freshwater flow with episodic wind-waves), and 2) summer conditions (low freshwater flow and steady diurnal wind-waves). The four-week period contains tidal variability due to the 14-day spring-neap cycle, which is critical for sediment transport processes. The center of the winter modeling period is determined as the time of peak sediment load ( $t_2$ , Figs. 9, 10), and two weeks are modeled before and after the peak. The fluxes are extrapolated for the time between elevated freshwater flow in the fall ( $t_1$ ), and the return to baseline summer flow ( $t_3$ ). The net sediment flux is then multiplied by a factor of 1/3, as this is the most dynamic period (the remainder of the winter is less dynamic). The beginning of the summer period is identified as the time at which baseline flows return ( $t_3$ ), to the end of the water year ( $t_5$ ). The temporal center is identified ( $t_4$ ), and two weeks before and after are modeled. The same extrapolations are performed for the summer period.

### Construction of flow and sediment load boundary conditions for 1867-1959

Sediment load data are available for the upstream boundaries of the domain (Freeport and Vernalis on the Sacramento and San Joaquin Rivers, respectively) for periods beginning in 1959. Hindcasting simulations require sediment load data for 1867-1990, therefore a method must be found to estimate daily sediment loads for 1867-1959. The first step is acquiring freshwater flow data.

#### *Determination of total yearly flow*

The eight-river index (California Department of Water Resources) is a measure of unimpaired flow into the Delta, and prior to water exports this represents the total flow into the Delta. This record is available back to 1906. Meko et al. (2001) developed a yearly time-series of total Sacramento River and San Joaquin flow using tree-ring chronologies, for the period 868-1977. This provides an estimate of total flows for 1867-1906.

### *Construction of monthly hydrograph*

Monthly total flows are available from the eight-river index, though combined values are provided for October/November, June/July, and August/September. Flow was split evenly between months with shared total flows. The monthly flows were compared with monthly precipitation totals from Sacramento, which span 1878-present. The total flow in a month was linearly regressed against the prior precipitation in the water year, for example, total January flow was regressed against total precipitation from October, November, December, and January. The regression spans 1906-1929, prior to major water diversions, when the eight-river index was a good measure of flow into the Delta. Using the regression equation with 1877-1906 precipitations data yields monthly flow estimates from 1877-1906.

### *Comparison of monthly hydrographs*

It is assumed that two years with similar monthly hydrographs share similar daily hydrographs. Therefore, the shape of monthly hydrographs from 1877-1928 were compared to monthly hydrographs from the period 1929-present, where daily data are available. For example, the monthly hydrograph from water year 1890 was cross-correlated with each of the 75 hydrographs from 1929-2003. The hydrograph from 1929-2003 that matched the 1890 shape closest was selected as the corresponding year, say, 1945. The daily hydrograph from 1945 was then used as the daily hydrograph for 1890. Multipliers were applied, if necessary, to maintain the same total flow as estimated from prior steps.

### *Comparison of yearly total flow*

For the period 1867-1877 there are limited precipitation data, so the total yearly flow was compared with the total yearly flow from 1929-2003. The year with the closest total flow was used as the surrogate daily hydrograph. Again, total flow was maintained.

### *Estimation of sediment loads*

The sediment rating curve relationship  $QC=aQ^b$ , was used to estimate sediment loads. The coefficient “b” (represents the erosive stream power) was determined using 2000-2003 data, with a value of 1.13. Coefficient “a” represents the sediment supply, and was used as the calibration parameter. Calibration data are from Gilbert (1917) (7.4 Mt/y, for 1849-1914) and Porterfield (1980) (3.5 Mt/y for 1909-1966). While these numbers are period averages, coefficient “a” was modified to yield the same period averages using daily data. Both Gilbert (1917) and Porterfield (1980) provide volumetric load estimates, these were converted to mass load estimates using an average density of  $529 \text{ kg/m}^3$  (Krone 1979).

## **Results**

### Calibration to water year 1997 fluxes

Model results (Fig. 7) compared well with sediment flux estimates as computed by McKee et al. (2006) and Ganju and Schoellhamer (in press). The seasonal pattern of sediment flux was represented, with export during high flows and import during the summer low-flow season. The net sediment export for 1997 was estimated at 2.83 Mt by Ganju and Schoellhamer (in press), while the model results show a net export of 2.74 Mt.

### Validation to water year 2004 fluxes

Preliminary model results (Fig. 8) compared well with sediment flux estimates as computed by McKee et al. (2006) and Ganju and Schoellhamer (in press) in terms of the seasonal pattern, with export during high flows and import during the summer low-flow season. However, the net sediment import for 2004 was estimated at 0.006 Mt by Ganju and Schoellhamer (in press), while the model results show a net export of 2.35 Mt. This discrepancy is attributed to poor agreement in the low-flow season, when landward dispersive flux is maximized. During this season, fluxes are extremely sensitive to the synthetic seaward sediment boundary condition. Future efforts will refine this boundary condition, especially for dry years.

### Formulation of time-stepping method

The two-season time-stepping method results in a net export of 2.96 Mt for 1997 as compared to the actual result of 2.74 Mt (Fig. 9). These small deviations are minimal, and suggest that this time-stepping procedure is suitable for decadal-scale simulations, where computational expense must be minimized.

### Construction of flow and sediment load boundary conditions for 1867-1959

A daily hydrograph was successfully constructed (Fig. 10, tile 1) and applied to the sediment load rating curve. Coefficient “a” was varied to obtain agreement with period loads estimated by Gilbert (1917) and Porterfield (1980) (Fig. 10, tile 2). These flow and sediment load time-series (Fig. 10, tile 3) may now be used in combination with the time-stepping method to perform the hindcasting simulations. Future changes in watershed sediment yield (due to land use change) may be implemented using the sediment rating curve.

## **Conclusions**

Without sediment flux or bathymetric change data, models of geomorphic change in an estuary cannot be accurately developed or evaluated. The data provided by McKee et al. (2006) and Ganju and Schoellhamer (in press) allow for the development of an idealized hydrodynamic/sediment transport model that is able to reproduce the seasonal patterns of sediment transport, both a dry and wet water year. This idealized model can now be utilized to both hindcast bathymetric change data for the period 1867-1990 (Cappiella et al., 1999), and evaluate geomorphic response to future climate change

scenarios. An idealized time-stepping method, which reduces the simulation time to four two-week periods, decreases computational time though error is introduced by this simplification. Reconstruction of landward flow and sediment load boundary conditions back to 1867 allows for the use of the time-stepping method in conjunction with the idealized model. Once the fully calibrated model successfully hindcasts the geomorphic change of the 19<sup>th</sup> and 20<sup>th</sup> centuries, it can be used with confidence to evaluate future scenarios of geomorphic change. The scenarios that will be evaluated include accelerated sea level rise, extended drought periods, and increased warming (leading to reduced snowpack). The outcome of the geomorphic modeling will help biologists and managers evaluate the effect of climate change on habitat availability, contaminant fate, and sediment transport in the 21<sup>st</sup> century.

## References

Arthur, J.F., Ball, M.D. 1979, Factors influencing the entrapment of suspended material in the San Francisco Bay-Delta Estuary, in Conomos, T.J. (ed), San Francisco Bay: the urbanized estuary, Pacific Division of the American Association for the Advancement of Science, San Francisco, p. 143–174.

Caffrey, J.M., Grenz, C., Cloern, J.E., 1998, Changes in production and respiration during a spring phytoplankton bloom in San Francisco Bay, California, USA: implications for net ecosystem metabolism, Marine Ecology Progress Series, 172, p. 1–12.

Cappiella, K., Malzone, C., Smith, R., Jaffe, B., 1999, Sedimentation and bathymetry changes in Suisun Bay, 1867-1990, U.S. Geological Survey Open-File Report 99-563.

Cloern, J.E., Cole, B.E., Wong, R.L.J., Alpine, A.E., 1985, Temporal dynamics of estuarine phytoplankton: A case study of San Francisco Bay, Hydrobiologia, 129, p. 153–176.

Coastal Engineering Research Center, 1984, Shore Protection Manual, U.S. Army Corps of Engineers, Waterways Experiment Station, Vicksburg, Mississippi.

Conomos, T.J., Peterson, D.H., 1977, Suspended-particle transport and circulation in San Francisco Bay: an overview, in Wiley, M. (ed.), Estuarine Processes, Academic Press, New York, 2, p. 82–97.

Gilbert, G.K., 1917, Hydraulic mining debris in the Sierra Nevada, U.S. Geological Survey Professional Paper 105, 148 pp.

Ganju, N.K. and Schoellhamer, D.H., 2005, Lateral displacement of the estuarine turbidity maximum in tidal strait, Proceedings of the 8th International Conference on Cohesive Sediment Transport, Saga, Japan, September 20-23, 2005.

Ganju, N.K., Schoellhamer, D.H., in press. Annual sediment flux estimates in a tidal strait using surrogate measurements, Estuarine, Coastal, and Shelf Science.

Goals Project, 1999, Baylands Ecosystem Habitat Goals. A report of habitat recommendations prepared by the San Francisco Bay Area Wetlands Ecosystem Goals Project. U.S. Environmental Protection Agency, San Francisco, Calif./S.F. Bay Regional Water Quality Control Board, Oakland, Calif.

Goodwin, P., Denton, R.A., 1991, Seasonal influences of the sediment transport characteristics of the Sacramento River, California, Proceedings of Institute of Civil Engineers, 2 (91), p. 163–172.

Jassby, A.D., Kimmerer, W.J., Monismith, S.G., Armor, C., Cloern, J.E., Powell, T.M., Schubel, J.R., Vendliniski, T., 1995, Isohaline Position as a Habitat Indicator for Estuarine Populations, Ecological Applications, 5 (1), p. 272–289.

Jassby, A.D., and Powell, T.M., 1994, Hydrodynamic influences on interannual chlorophyll variability in an estuary: Upper San Francisco Bay-Delta (California, U.S.A.): Estuarine, Coastal and Shelf Science, v. 39, p. 595-618.

Kimmerer, W.J., 1992, An evaluation of existing data on the entrapment zone of the San Francisco Bay estuary. Interagency Ecological Studies Program, Sacramento, Technical Report

Krone, R.B., 1979, Sedimentation in the San Francisco Bay system, In San Francisco Bay: The Urbanized Estuary (Conomos, T.J., ed), p. 85-96, Pacific Division of the American Association for the Advancement of Science, San Francisco, California.

McKee, L.J., Ganju, N.K., Schoellhamer, D.H., 2006, Estimates of suspended sediment flux entering San Francisco Bay from the Sacramento and San Joaquin Delta, San Francisco Bay, California, Journal of Hydrology, 323, 335-352.

Peterson, D.H., Conomos, T.J., Broenkow, W.W., and Doherty, P.C., 1975, Location of the non-tidal current null zone in northern San Francisco Bay: Estuarine and Coastal Marine Science, v. 3, p. 1-11.

Pont, D., Day, J.W., Hensel, P., Franquet, E., Torre, F., Rioual, P., Ibanez, C., and Coulet, E., 2002, Response scenarios for the deltaic plain of the Rhone in the face of an acceleration in the rate of sea-level rise with special attention to *Salicornia*-type environments: Estuaries, v. 25, no. 3, p. 337-358.

Porterfield, G., 1980, Sediment transport of streams tributary to San Francisco, San Pablo, and Suisun Bays, California, 1909-1966. U.S. Geological Survey Water Resources Investigations, 80-64.

Ruhl, C.A., Schoellhamer, D.H., 2004, Spatial and temporal variability of suspended-sediment concentrations in a shallow estuarine environment, San Francisco Estuary and Watershed Science, 2(2), article 1.

Scavia, D., Field, J. C., Boesch, D.F., Buddemeier, R. W., Cayan, D.R., Burkett, V.,

Fogarty, M., Harwell, M., Howarth, R., Mason, C., Reed, D.J., Royer, T.C., Sallenger, A.H., and Titus, J.G., 2002, Climate change impacts on U.S. coastal and marine ecosystems: *Estuaries*, v. 25, p.149-164.

Schoellhamer, D.H., 2001a, Influence of salinity, bottom topography, and tides on locations of estuarine turbidity maxima in northern San Francisco Bay, in McAnally, W.H. and Mehta, A.J. (eds.), *Coastal and Estuarine Fine Sediment Transport Processes*, Elsevier Science B.V., p. 343–357.

Schoellhamer, D.H., 2001b, Singular spectrum analysis for time series with missing data: *Geophysical Research Letters*, v. 28, no. 16, p. 3187-3190.

Schoellhamer, D. H., Burau, J. R., 1998, Summary of findings about circulation and the estuarine turbidity maximum in Suisun Bay, California, U.S. Geological Survey Fact Sheet FS-047-98. 6 pp.

Shchepetkin, A.F. and McWilliams, J.C., 2005, The Regional Ocean Modeling System (ROMS): A split-explicit, free-surface, topography-following coordinates ocean model, *Ocean Modelling*, 9, 347-404.

Warner, J.C., Geyer, W.R., and Lerczak, J.A., 2005. Numerical modeling of an estuary: a comprehensive skill assessment, *Journal of Geophysical Research*, 110, C050001.

Wright, S.A., and Schoellhamer, D.H., 2004, Trends in the sediment yield of the Sacramento River, California, 1957-2001, *San Francisco Estuary and Watershed Science*, 2(2), article 2.

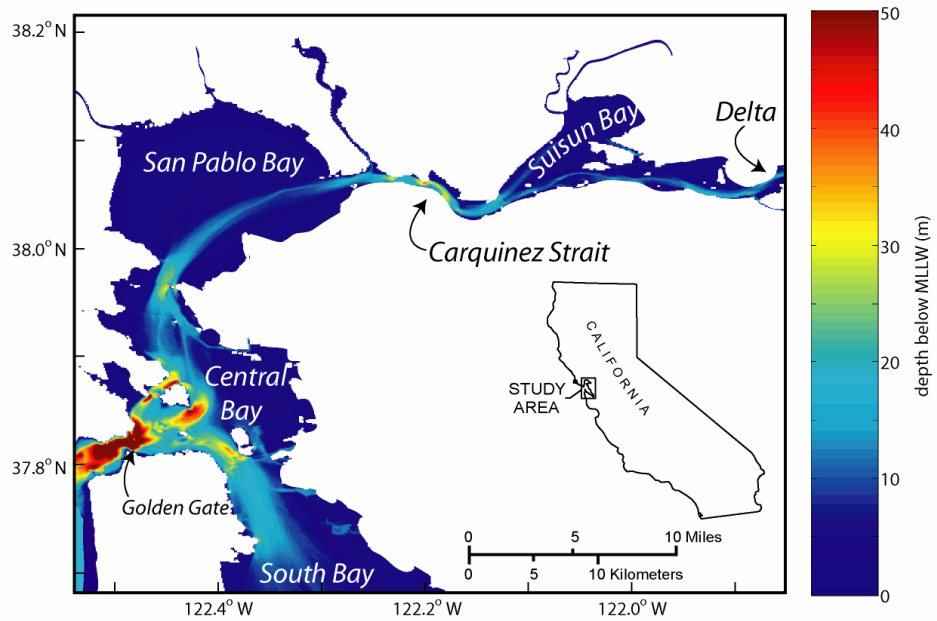


Figure 1. San Francisco Bay and western end of Sacramento/San Joaquin River Delta. Suisun Bay is upstream-most embayment of San Francisco Bay.

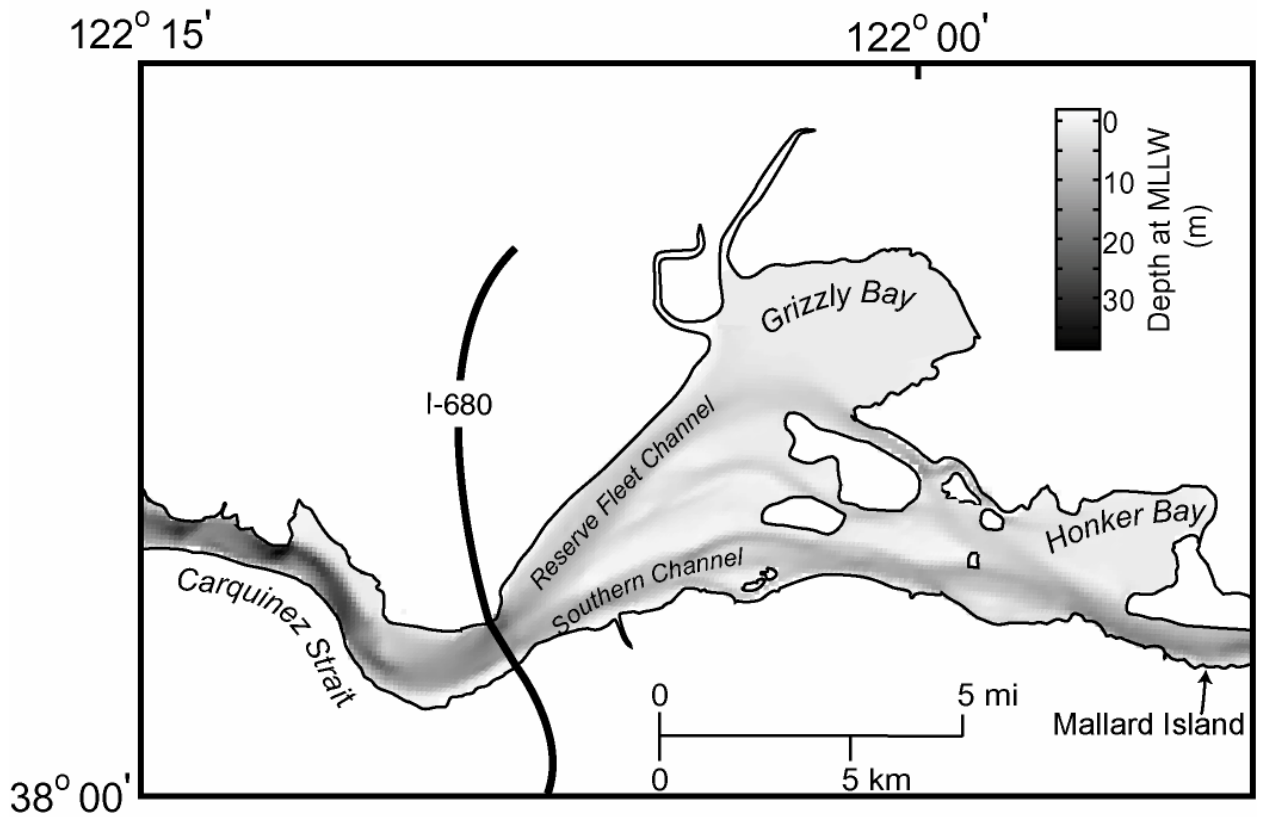


Figure 2. Suisun Bay and Carquinez Strait. Carquinez Strait connects San Pablo Bay and Suisun Bay. Sites NBen and SBen are located on piers of the I-680 Bridge.

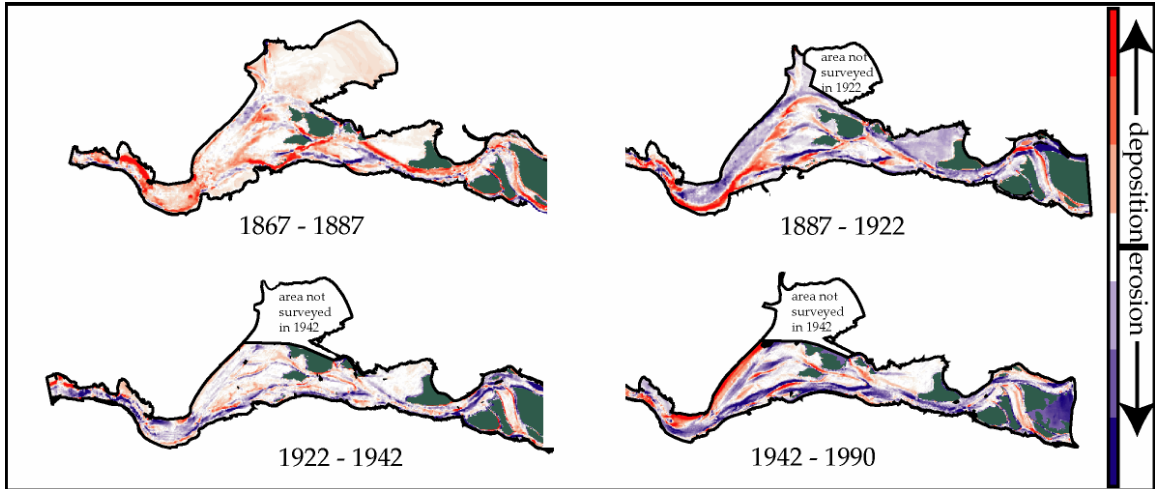


Figure 3. Bathymetric change in Suisun Bay, from Cappiella et al. (1999). Red areas are erosional, purple areas are depositional. Deposition was greatest between 1867 and 1887, when hydraulic mining debris was transported into Suisun Bay from the watershed.

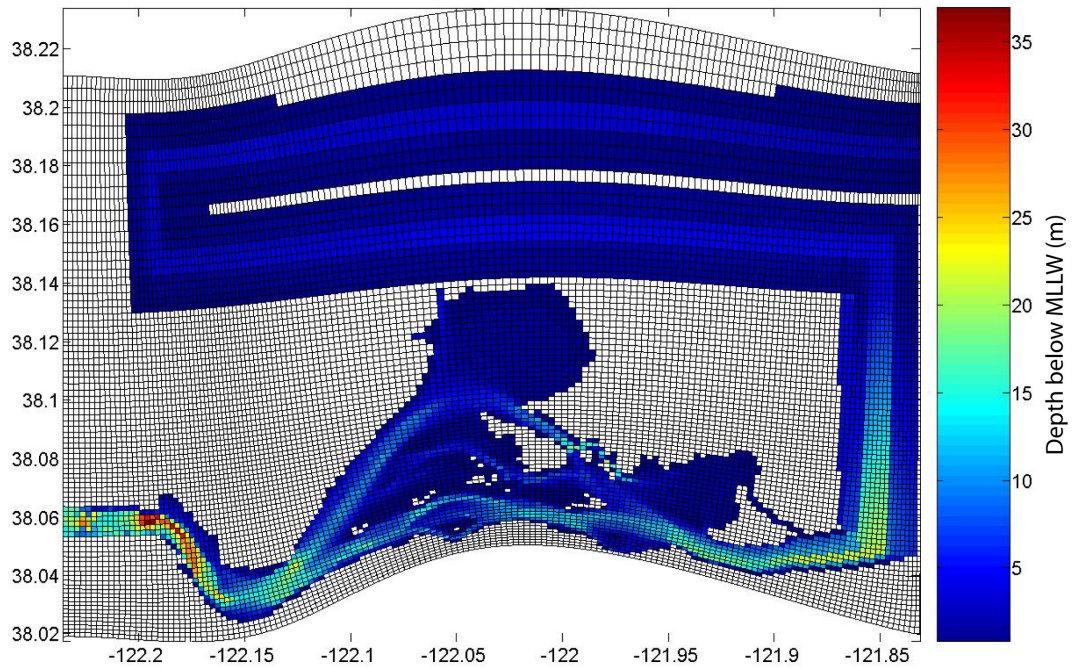


Figure 4. Modeling domain of Suisun Bay. The Sacramento/San Joaquin Delta has been idealized as a trapezoidal channel, with the same area as the Delta and same length of the Sacramento River to Freeport.



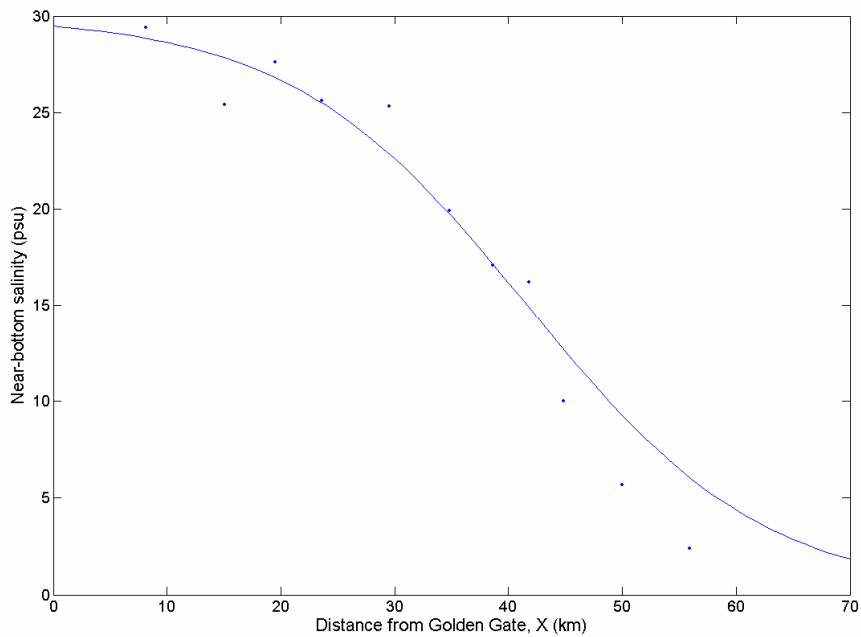


Figure 5. Example of R/V Polaris cruise data (points) and empirical fit of Equation 1 (line). This fitting procedure was repeated for 358 Polaris cruises to determine values for  $\beta$  as a function of freshwater flow. For this example,  $\beta=20.8$ . Dayflow for this period was  $283 \text{ m}^3/\text{s}$ .

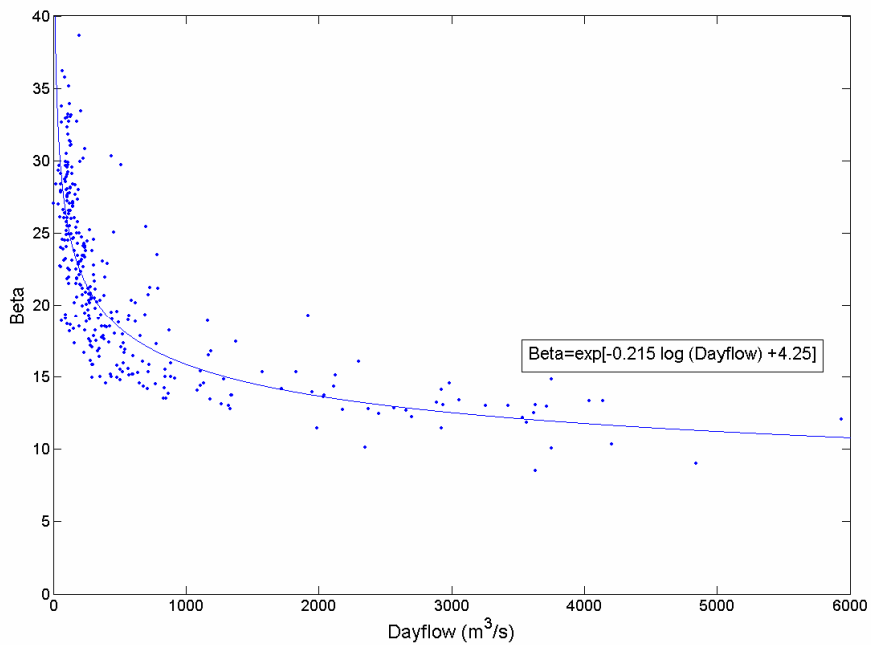


Figure 6. Variation of parameter beta with freshwater outflow. Exponentially decaying fit is implemented into the model to calculate flood-tide salinity.

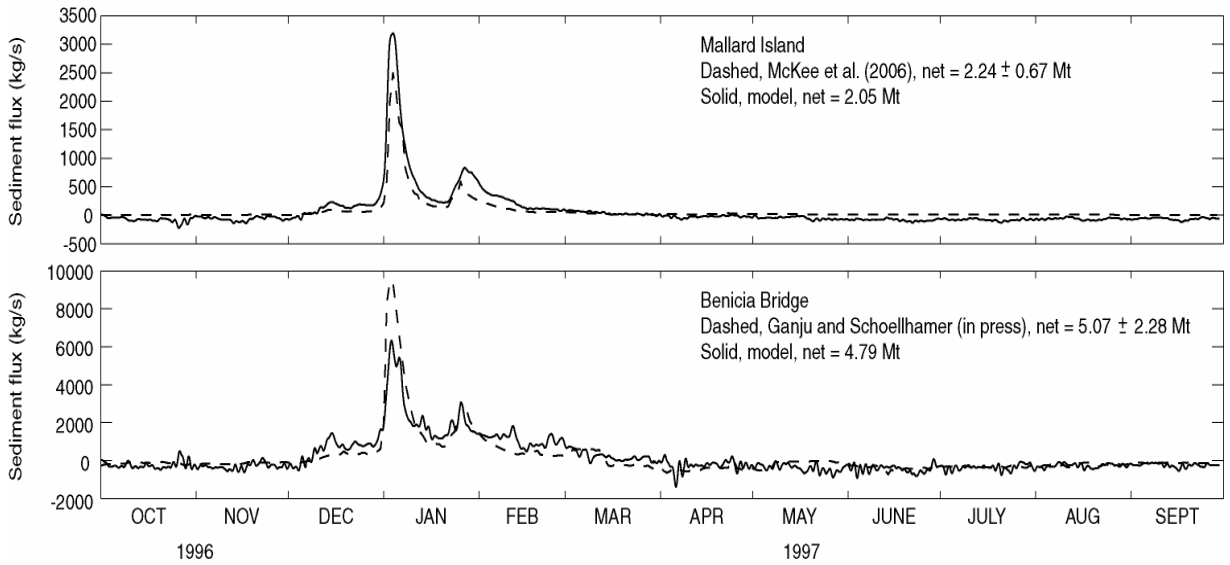


Figure 7. Sediment flux estimates and model simulations for water year 1997. Positive values indicate seaward transport.

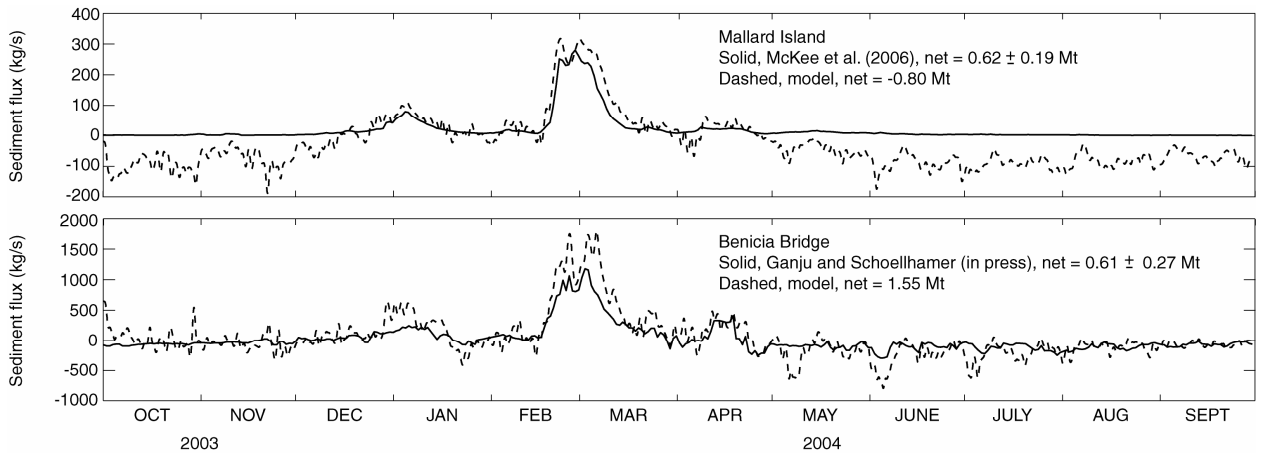


Figure 8. Sediment flux estimates and model simulations for water year 2004. Positive values indicate seaward transport.

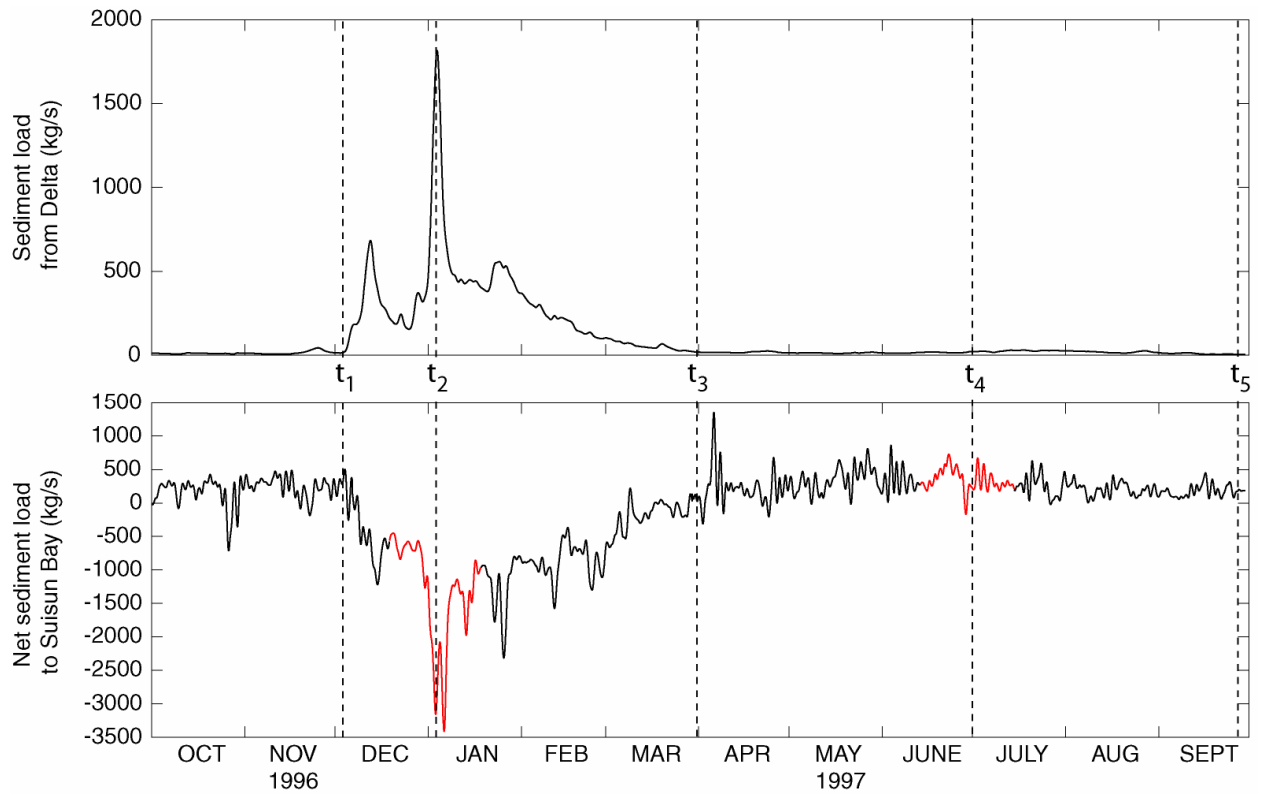


Figure 9. Illustration of time-stepping method, for water year 1997. Two four-week periods (red) are identified as peak winter and summer periods based on sediment load from the Delta; these periods are simulated and extrapolated to represent the entire year.

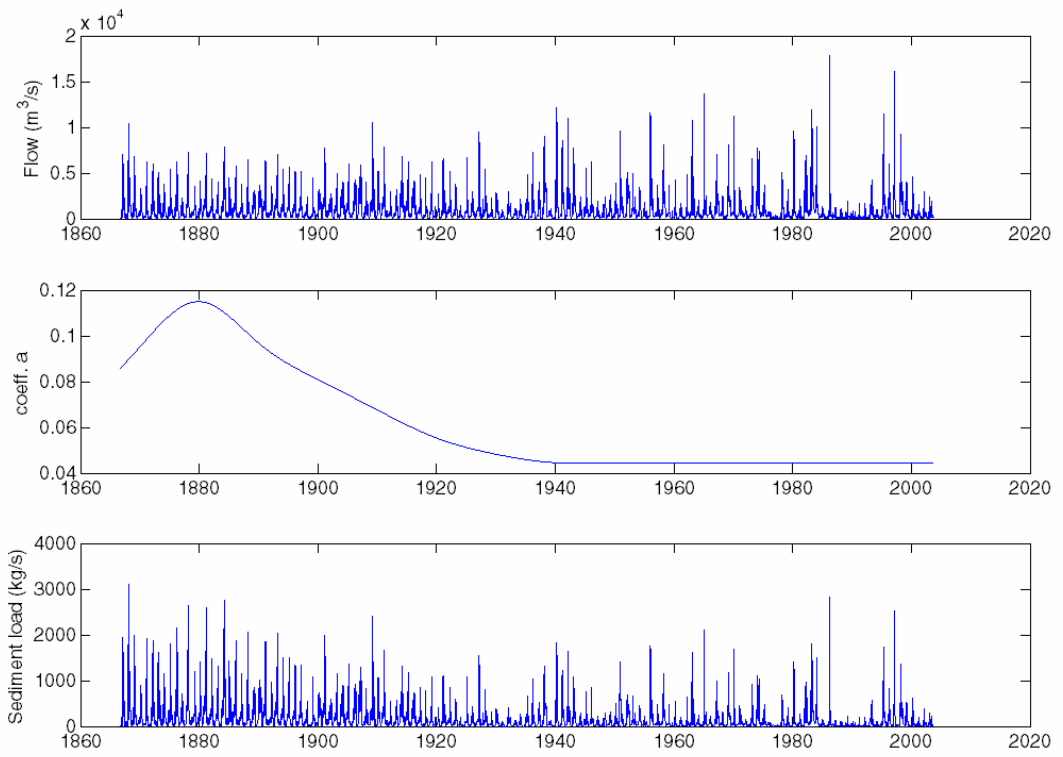


Figure 10. Reconstructed daily hydrograph, calibrated coefficient “a”, and daily sediment load time-series for 1867-present.